International Journal of Soft Computing and Engineering (IJSCE)
ISSN: 2231-2307, Volume-2 Issue-1, March 2012

Reconstruction of Shape and Position for Scattering Objects by Linear Sampling Method

A.R. Eskandari, M. Naser-Moghaddasi, M. Eskandari

Abstract— This paper presents an approach for shape and position reconstruction of a scattering object using microwaves where the scatterer is assumed to be a homogenous dielectric medium. The employed technique assumes no prior knowledge of the scatter's material properties like electric permittivity and conductivity, and the far-field pattern is used as the only primary information in identification. The approach proposed consists of retrieving the shape and the position of the scattering object using a linear sampling method. The technique results in high computational speed and efficiency. In addition, the technique can be generalized for any scatterer structure. Numerical results are used to validate the feasibility of the proposed approach.

Index Terms— Shape Reconstruction, Inverse Scattering, Microwave Imaging, Linear Sampling Method (LSM).

I. INTRODUCTION

Reconstruction of an electromagnetic (EM) scatterer is a special case of target identification. The imaging of scattering objects using microwaves is a major problem which is intensely investigated in the field of science and technology. This kind of imaging is implemented using an electromagnetic inverse scattering technique which involves the determination of geometrical and physical properties of a scatterer, such as position, size, shape, permittivity, conductivity, and permeability, from the measurements of the scattered EM fields resulting from the interaction of known incident waves with the unknown object [1], [2], as illustrated in Fig.1.

microwave imaging has many applications ranging from nondestructive testing and evaluation to medical imaging, and from civil engineering to target identification [3]-[5], the importance of solving the inverse EM problem to determine the shape and location of an object has become paramount. Even though this problem is not fairly new as we can refer to x-ray imaging in the early 20th century, however the complexity of EM imaging has hindered the exact and precise solution [6], [7] because of ill-posedness and nonlinearity. What is meant by ill-posedness is that one of the following conditions is not satisfied: the existence of the solution; the uniqueness of the solution; or the continuity of the inverse mapping. For these reasons robust analytical tools involving the use of computationally intensive techniques are required. The various techniques employed are different according to the model used to define the scattering object, such as material properties and boundary conditions, and method of determining the solution. In this paper the scatterer is considered homogenous, electromagnetically penetrable, located in free space. The goal of the proposed technique was to reconstruct the scatterer's profile and position.

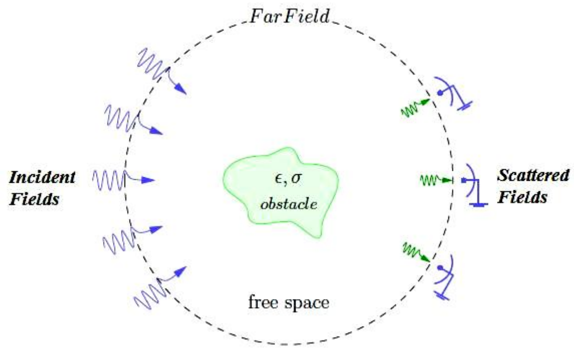

Fig.1 Incident and scattered fields configuration in the model of inverse scattering problem.

Since microwave imaging has many applications ranging from nondestructive testing and evaluation to medical imaging, and from civil engineering to target identification [3]-[5], the importance of solving the inverse EM problem to determine the shape and location of an object has become paramount. Even though this problem is not fairly new as we can refer to x-ray imaging in the early 20th century, however the complexity of EM imaging has hindered the exact and precise solution [6], [7] because of ill-posedness and nonlinearity. What is meant by ill-posedness is that one of the following conditions is not satisfied: the existence of the solution; the uniqueness of the solution; or the continuity of the inverse mapping. For these reasons robust analytical tools involving the use of computationally intensive techniques are required. The various techniques employed are different according to the model used to define the scattering object, such as material properties and boundary conditions, and method of determining the solution. In this paper the scatterer is considered homogenous, electromagnetically penetrable, located in free space. The goal of the proposed technique was to reconstruct the scatterer's profile and position.

Numerical methods employed for solving inverse scattering problems can be grouped into two categories, i.e. qualitative and

Manuscript Received Feb. 2012

A.R. Eskandari, Department of Engineering, East Tehran Branch, Islamic Azad University, Tehran, Iran, Phone No.: +98-2133584912 (e-mail: ar_eskandary@yahoo.com)

M. Naser-Moghaddasi, Faculty of Eng., Science and Research Branch, Islamic Azad University, Tehran, Iran.
(e-mail: mn.moghaddasi@srbiau.ac.ir)

M. Eskandari, Electrical and Computer Engineering Department, Isfahan University of Technology, Isfahan, Iran (e-mail: mr.eskandari@ec.iut.ac.ir)

quantitative approaches. The singular sources [8], [9], the factorization method (FM) [4], [10] and the sampling method (SM) or the linear sampling method (LSM), are examples of qualitative methods. The LSM, introduced by D. Colton and A. Kirsch [11], is an effective method to tackle the problem of reconstructing the shape of the unknown scatterer. This method does not require a priori knowledge on the scatterer's profile, however the physical properties, such as electrical permittivity value, of a penetrable scatterer cannot be calculated by using it [7], [11]-[16]. There are also various quantitative methods used to reconstruct the scatterer, i.e. the nonlinear and linear approximation methods. Although these methods are capable of reconstructing the scatterer with high precision unfortunately they require a great deal of iterations to improve the initial guess [7], [11] and thus are very time consuming. In this paper, the LSM approached is used for reconstruction because the many advantages aforementioned.

The paper is organized as follows. In Section II, an appropriate model for the direct problem is introduced. In Section III, the mathematical details and the general formulations of LSM are described. The numerical examples are given in Section IV. Finally, Section V draws some conclusions.

II. DIRECT SCATTERING

In order to solve any inverse problem there has to be an appropriate model for the direct problem. In the direct scattering problem the scatterer and incident field are known quantities. The problem is to compute the scattered field in the form of a far-field pattern. For this scenario the Maxwell equations are defined by:

$$\nabla \times \vec{\boldsymbol{E}} + \mu \frac{\partial \vec{\boldsymbol{H}}}{\partial t} = 0 \qquad (1a)$$

$$\nabla \times \vec{\boldsymbol{H}} - \varepsilon \frac{\partial \vec{\boldsymbol{E}}}{\partial t} = 0 \qquad (1b)$$

where $\vec{\boldsymbol{E}}$ and $\vec{\boldsymbol{H}}$ are electric and magnetic fields, ε is the electric permittivity and μ is the magnetic permeability. If the electric and magnetic fields are time harmonic with ω frequency, equation (1) is represented by:

$$\nabla \times \vec{\mathrm{E}} + i\omega\mu\vec{H} = 0 \qquad (2a)$$

$$\nabla \times \vec{H} - i\omega\varepsilon\vec{E} = 0 \qquad (2b)$$

Assume that D is the homogenous penetrable scatterer in R^3 space. With this presumption the inhomogeneous R^3 space will be divided to two homogeneous regions of D and $R \setminus D$. Considering that the structure of the scatterer is infinite in one direction (z-axis) and the incident electric field is polarized parallel to the same infinite dimension of the object (TM polarization), the components of the $\vec{E}$ and $\vec{H}$ fields can be simplified as:

$$\vec{E} = (0, 0, u) \qquad (3a)$$

$$\vec{H} = \frac{1}{i\omega\mu}\left(\frac{\partial u}{\partial y}, -\frac{\partial u}{\partial x}, 0\right) \qquad (3b)$$

in which u is the only component of the electric field. This equation shows that all of the components of the $\vec{E}$ and $\vec{H}$ can be found by using u. Therefore, from this point on the electric field will be considered the same as u. If the internal electric field is u^{int} on the D region and the external electric field is u^{ext} on the $R^2 \setminus D$ region, by using the Maxwell equations, the scalar wave will be given by:

$$\nabla^2 u^{\text{int}} + k^2 \zeta u^{\text{int}} = 0 \quad on \quad D \qquad (4)$$

$$\nabla^2 u^{ext} + k^2 u^{ext} = 0 \quad on \quad R^2 \setminus \overline{D} \qquad (5)$$

where k is the wave number of free space and is defined as $k = 2\pi/\lambda$. Since the scatterer is lossy, the relative complex permittivity is determined as $\zeta = \varepsilon_r - i\varepsilon_r'$, in which the imaginary section of [illegible] is calculated from the following equation:

$$\varepsilon_r' = \sigma/\omega\varepsilon_0 \qquad (6)$$

In the above equation, σ is the electric conductivity, and ε_0 is the electric permittivity of free space. As mentioned before, it can be said that the incident field is a plane wave in the direction of $\hat{d} \in \Omega$,

$$u^i = e^{-ik\hat{x}.\hat{d}} \qquad (7)$$

and the external electric field is the total of the incident field (u^i) and the scattered field (u^s),

$$u^{ext} = u^i + u^s \qquad (8)$$

The existence of boundary conditions in all of the R^2 space is one of the conditions that may lead to the well-posedness of a scattering problem and complete the model of the problem. These conditions include the discontinuity of region on ∂D and the Sommerfeld radiation condition. Therefore,

$$u^{ext}\Big|_{\partial D^+} = u^{\text{int}}\Big|_{\partial D^-} \qquad (9a)$$

$$\left.\frac{\partial u^{ext}}{\partial n}\right|_{\partial D^+} = \left.\frac{\partial u^{\text{int}}}{\partial n}\right|_{\partial D^-} \qquad (9b)$$

The Sommerfeld radiation condition for the scattered field is defined as:

$$\lim_{|\vec{x}| \to \infty} \sqrt{\vec{x}} \left(\frac{\partial u_s}{\partial |\vec{x}|} + iku_s\right) = 0 \qquad (10)$$

According to aforementioned points, it could be said that equations (4), (9), and (10) are a complete mathematical model of the direct scattering problem for the scatterer D, for which if the incident field is known, the scattered field will be calculated as u_s.

Since the precision and accuracy of the measured scattered field are high in far-field zones, solving the inverse scattering problem is implemented in this zone. Though, we are able to study this problem for scattered fields in near-field zones from the scatterer. It should be mentioned that in dealing with the ill-posedness problem, the latter approach is somewhat easier than the former one. For this reason, to solve a problem in far-field zone the pattern of the far-field is determined via the symbol u^{∞}. Any scattering problem which satisfies the Helmholtz equations has asymptotic behavior outside of the scatterer which is $R\setminus D$. By using the Sommerfeld radiation condition and the Green integral equation, we have:

$$u_s(\vec{x},\hat{d})=\frac{e^{-ik|\vec{x}|}}{\sqrt{|\vec{x}|}}\left(u^{\infty}(\hat{x},\hat{d})+o\left(\frac{1}{|\vec{x}|}\right)\right) \qquad (11)$$
$$|\vec{x}|\to\infty$$

for which u^{∞} represents the far-field pattern and $\hat{x}$ is cylindrical unit vector in Ω space.

III. INVERSE SCATTERING (LINEAR SAMPLING METHOD)

Our primary purpose is to reconstruct the shape of the scatterer by assuming a known far-field pattern u^{∞} for every $\hat{x},\hat{d}\in\Omega$ and constant wave number k. In the range of the resonance frequency the problem is solved using a sampling method. The principle of this technique is based on solving the Fredholm integral equation of the first kind ($Fg=\phi$), as follow

$$(12)\ \mathrm{F}g(\hat{\mathrm{x}})=\int_{\Omega}u_{\infty}(\hat{x},\hat{d})g(\hat{d})d\Gamma(\hat{d})=e^{ik\hat{x}.\hat{d}},\ \hat{x}\in\Omega$$

in which F is known as the far-field operator and u_{∞} is the far-field pattern for the incident wave $u^{i}=e^{-ikxz}$. A question that maybe raised is why and how the integral equation $Fg=\phi$ and finding g will help to reconstruct the shape and the position of the scatterer D. Actually, Colton [13] showed that if $g_{\varepsilon}(.,\vec{z})$ would be a good approximation for g, for every $\varepsilon>0$, we could have:

$$(13)\ \|Fg_{\varepsilon}(.,\vec{z})-\phi(.,\vec{z})\|<\varepsilon$$

then for $z\in D$, we can say:

$$(14)\ \lim_{\vec{z}\to\partial D}\|g_{\varepsilon}(.,\vec{z})\|_{L^2(\Omega)}=\infty\ , \qquad \vec{z}\in D$$

and we can say that for $z\in R\setminus\overline{D}$, the equation $\|g_{\varepsilon}(.,\vec{z})\|=\infty$ is established in general.

In summary, it can be said that if the chosen assumed point source is inside the scatterer $z\in D$, we can show the far-field pattern by using a spectrum of the incident wave with a amplitude g. But if this point source is located on or outside of the boundary $z\in R\setminus D$, the use of a spectrum of the incident wave with finite amplitude is not possible. For this very reason $\|g\|$ is infinite on or outside of the boundary. It should be mentioned that the above conditions are fully satisfied if the scattering problem is solved analytically and not numerically.

The errors caused by the discretization of the inverse problem will hinder viewing this event. As we approach the boundary ∂D from the inside of the scatterer the value of $\|g_{\varepsilon}\|$ will increase. This value is larger on the outside of the scatterer $R\setminus\overline{D}$. But this does not mean that the increasing process of $\|g_{\varepsilon}\|$ is ascending. In fact, in some paths the value may decrease, but in comparison with the inside of the scatterer the value is very large and it can be said that $\|g_{\varepsilon}\|$ is a specification function for D.

According to what has been said our goal in this section is to solve the integral equation $Fg=\phi$. But because of the smoothness of this integral equation's kernel u^{∞}, the numerical realization of it is considered as an ill conditioned linear problem. The differences of the sampling methods are exact in solving this integral equation. LSM, which was first introduced but Colton and Kirsch [11] in 1996, is amongst the first methods of the group of sampling methods. In this method, the problem is changed in a way so that the ill-posedness of it decreases so that it can also be a good approximation for the unknown scatterer. In other words, it can be said that the goal is to minimize the error function shown below:

$$(15)\ \|Fg_{\varepsilon}(.,\vec{z})-\phi(.,\vec{z})\|^2+\alpha\|g_{\varepsilon}(.,\vec{z})\|^2$$

In this equation α is the Tikhonov regularization parameter. The smaller the α value, the closer the answer of the error function of the extremum problem gets to the real value. But if it's too small or in other words if $\alpha=0$ it will cause the problem to go back to its ill-posed condition. The larger the α value, the smoother and simpler the solution of ill-posed problem. But if it's too large, the answer will be distance from the actual answer. For this reason an optimum value has to be chosen for α. Various methods exist for choosing α including Morozov's discrepancy principle and L-curve [17]-[19] in which by choosing this parameter α the value of g and hence $\|g\|$ will be obtained eventually. One of the methods for solving the integral equation (12) is the factorization method. In [17], Kirsch proved that if the chosen point source is inside the scatterer $z\in D$, the far-field function $\phi(.,z)$ will be in the range of $(F^{*}F)^{1/4}$ operator. This conclusion will be a kind of range identity for the primary integral equation. For further information, refer to reference [10].

IV. NUMERICAL RESULTS

In this section the numerical results of different 2D structures will be presented. In all of the results presented the physical dimensions and distances have been normalized according to wavelength scale. The algorithm applied by the means of LSM the shape and the position of the scatterers are reconstructed. In LSM, there is no need to solve the direct problem, but the far field pattern is the input data of this problem. Therefore, the direct problem has to be solved according to the number of incident waves. To decrease the amount of computations in this stage one incident wave is used. The sampling points have been chosen in the $\{(x, y) \in R^2 : 0 < x < 1 \, , \, 0 < y < 1\}$ region. The grid has been obtained uniformly by discretizing the region into 101×101 points.

In the simulation, sampling has been done uniformly on the far-field pattern. The far-field pattern is computed for the case where the number of the incident angles is equal to 18 (0r 72), and their incident direction and measured direction are the same. Therefore:

$$k_i = k_s = [\cos(n\pi/18), \sin(n\pi/18)] \qquad (18)$$

Forward scattering data is produced by using an integral equation on the scatterer (D region). This integral equation is referred to in [20]. The produced fields from this integral equation are used in the LSM. In solving the mentioned integral equation, the moment method is used for discretization of the D region [20], [21]. The basic functions in our simulations are chosen to be a rectangular pulse. In all examples, the discretization is rectangular and the maximum value of the elements length is chosen to be $\lambda/10$.

The first example is relative to an aircraft-shaped scattering object, as shown in Fig. 2. This is a homogeneous dielectric scatterer which has a relative complex permittivity equal to $\zeta = 4 - j0.1$ ($\varepsilon_r = 4$, $\varepsilon_r' = 0.1$). Also, it is assumed that the wavelength of the incident field is equal to 20π ($\lambda = 20\pi$ or $k = 0.1$) and the number of the incident angles is equal to 18. The Tikhonov regularization parameter (α) is calculated by Morozov's discrepancy principle [18] and it is equal to 5.3×10^{-8}. Fig. 2 shows the result of the reconstructed shape of this scatterer qualitatively. In fact, the shape of the actual scatterer has been shown by a closed blue line. $\|g\|$ is a characteristic function of the target and the boundary of the shape can be reconstructed by drawing an appropriate level. Also by choosing a specification function like $f(.) = -\log(.)$, the image of $\|g\|$ ($f(\|g\|)$) can be drawn so that the shape of the scatterer could be clearer.

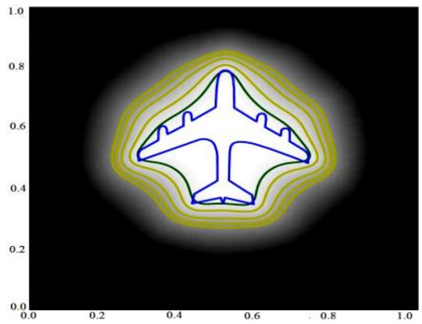

Fig. 2 Shape and position reconstruction of an aircraft-shaped scattering object with $\varepsilon_r = 4$ and $\varepsilon_r' = 0.1$ in free space by using LSM (*k=0.1*).

For the same example in Fig.3, shape and position reconstruction have been shown for higher frequencies. In Fig. 3(a), the wavelength of the incident field is equal to 4π ($\lambda = 4\pi$ or $k = 0.5$), and in Fig. 3(b) it is equal to 2π ($\lambda = 4\pi$ or $k = 0.5$). As this Figure shows, wherever the frequency of the incident field is closer to the resonance frequency, its reconstruction is more precise.

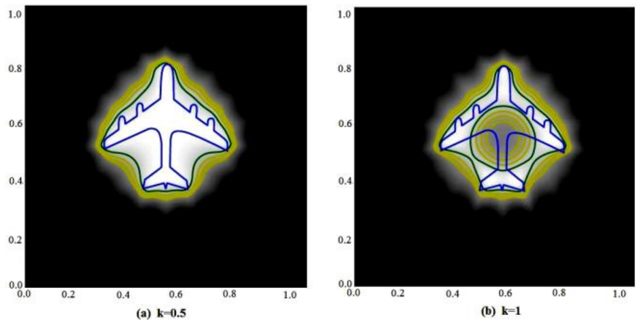

Fig. 3 Shape and position reconstruction of an aircraft-shaped scattering object by LSM (a) *k=0.5*, (b) *k=1*

The second example is relative to an I-shaped and a T-shaped scattering object, as shown in Fig. 4. This is a homogeneous dielectric scatterer which has a relative complex permittivity equal to $\zeta = 2 - j0.5$ ($\varepsilon_r = 2$, $\varepsilon_r' = 0.5$). Also, it is assumed that the wavelength of the incident field is equal to 2π ($\lambda = 2\pi$ or $k = 1$) and the number of the incident angles is equal to 18. The Tikhonov regularization parameter (α) is calculated by Morozov's discrepancy principle [18] and it is equal to 4.72×10^{-8}. Fig. 4 shows the result of the reconstructed shape of these scatterers qualitatively. In Fig. 5 and Fig. 6, the frequency of the incident wave is increased, such that the wavelength of the incident field is equal to 2 and 1 in Fig. 5 and Fig.6, respectively. In Fig. 7, the number of the incident angles is equal to 72. These figures show that by increasing the frequency of the incident wave and also by increasing the number of the incident angles, the precision of reconstruction becomes higher.

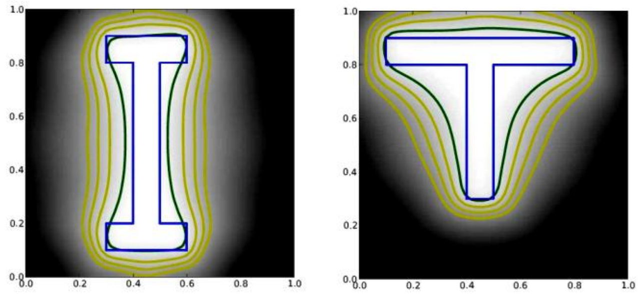

Fig. 4 Shape and position reconstruction of the scattering objects by LSM. (the number of the incident angles is equal to 18 and $k = 1$)

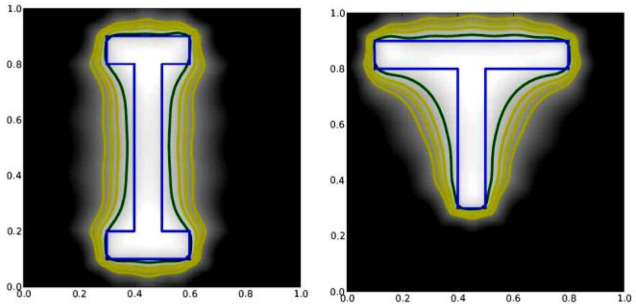

Fig. 5 Shape and position reconstruction of the scattering objects by LSM. (the number of the incident angles is equal to 18 and $k = \pi$)

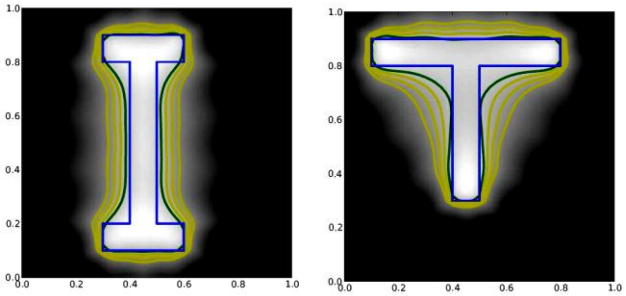

Fig. 6 Shape and position reconstruction of the scattering objects by LSM. (the number of the incident angles is equal to 18 and $k = 2\pi$)

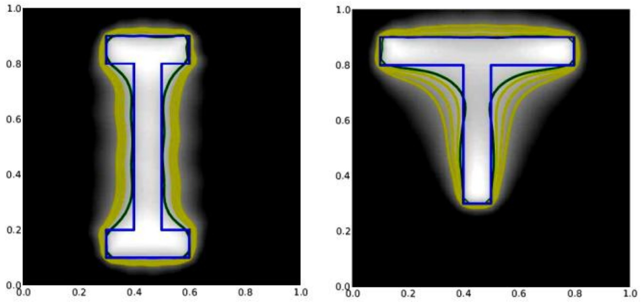

Fig. 7 Shape and position reconstruction of the scattering objects by LSM. (the number of the incident angles is equal to 72 and $k = 2\pi$)

V. CONCLUSION

Shape and position reconstruction of a scattering object at microwave frequency was described using the linear sampling method. The LSM was proposed because it can be applied to an extremely wide class of scatterers without any a priori information. The advantage of this approach is its high computational efficiency and speed. Furthermore, the approach described can be generalized for scatterer structures. Numerical results are used to validate the described technique. These results showed, wherever the frequency of the incident field is closer to the resonance frequency, and when the number of the incident angles increases, the reconstruction of the scatterer is more precise.

ACKNOWLEDGMENT

This research work has been financially supported by East Tehran Branch, Islamic Azad University, Tehran, Iran.

REFERENCES

1. Soldovieri, F., Brancaccio, A., Leone, G., and Pierri, R.: “Shape reconstruction of perfectly conducting objects by multiview experimental data”, IEEE Trans. Geosci. Remote Sens., 2005, 43, (1), pp.65-71.
2. Eskandari, M., and Safian R.: “Inverse scattering method based on contour deformations using a fast marching method”, Inverse Problems (IOP), 2010, 26, (9), 19.
3. Jin, T., and Zhou, Z.: “Refraction and dispersion effects compensation for UWB SAR subsurface object imaging”, IEEE Trans. Geosci. Remote Sens., 2007, 45, (12), pp.4059-4066.
4. Fischer, C., Herschlein, A., Younis, M., and Wiesbeck, W.: “Detection of antipersonnel mines by using the factorization method on multistatic ground-penetrating radar measurements”, IEEE Trans. Geosci. Remote Sens., 2007, 45, (1), pp. 85-92.
5. Benedetti, M., Donelli, M., Martini, A., Pastorino, M., Rosani, A., and Massa, A.: “An innovative microwave imaging technique for nondestructive evalution: Applications to civil structures monitoring and biological bodies inspection”, IEEE Trans. Instrum. Meas., 2006, 55, pp.1878-1884.
6. Li, G.H., Zhao, X., and Huang, K.M.: “Frequency dependence of image reconstruction of linear sampling method in electromagnetic inverse scattering”, Progress In Electromagnetics Research Symposium Proceedings, Xi'an, China, March 2010, pp.611-614.
7. Colton D., Haddar H., and Piana M.: “The linear sampling method in inverse electromagnetic scattering theory”, Inverse Problems (IOP), 2003, 19, (1), pp.105-137.
8. Potthast R.: “Stability estimates and reconstruction in inverse scattering using singular sources”, J. Comp. Appl. Math., 2000, 114, pp.247-274.
9. Fotouhi, M., and Hesaaraki, M.: “The singular sources method for an inverse problem with mixed boundary conditions”, Journal of Mathematical Analysis and Applications, 2005, 306, (1), pp.122-135.
10. Kirsch A.: “The factorization method for Maxwell's equations”, Inverse Problems, 2004, 20, (6), pp.117-134.
11. Colton, D., and Kirsch A.: “A simple method for solving inverse scattering problems in the resonance regions”, Inverse Problems, 1996, 13, pp.383-393.
12. Cakoni, F., and Colton, D.: Qualitative Methods in Inverse Scattering Theory, Berlin, Germany: Springer Verlag, 2006.
13. Cakoni, F., Colton, D., and Haddar, H.: “The linear sampling method for anisotropic media”, Journal of Computational and Applied Mathematics, 2002, 146, pp.285-299.
14. Catapano, I., Crocco, L., and Isernia, T.: “Improved sampling methods for shape reconstruction of 3-D buried targets”, IEEE Transaction on Geoscience and Remote Sensing, 2008, 46, (10), pp.3265-3273.
15. Cakoni, F., Colton, D., and Haddar, H.: “The linear sampling method for anisotropic media”, Journal of Computational and Applied Mathematics, 2002, 146, pp.285-299.
16. Cakoni, F., Colton, D., and Monk, P.: “The inverse electromagnetic scattering problem for a partially coated dielectric”, Journal of Computational and Applied Mathematics, 2007, 204, pp.256-267.
17. Bazan, F.S.V.: “Fixed-point iterations in determining a Tikhonov regularization parameter”, Inverse Problems, 2008, 24, pp.1-15.
18. Colton, D., Piana, M., and Potthast, R.: “A simple method using Morozov's discrepancy principle for solving inverse scattering problems”, Inverse Problem, 1999, 13, pp.1477-1493.
19. Pelekanos, G., and Sevroglou, V.: “Shape reconstruction of a 2D-elastic penetrable object via the L-curve method”, Journal of Inverse Ill-Posed Problems, 2006, 14, (4), pp.1-16.
20. Harrington, R. F.: Field Computations by Moment Methods, New York: MacMillan, 1968.
21. Gibson, W. C.: The Method of Moments in Electromagnetics, Chapman & Hall/CRC, 2008.